

000
001
002
003
004
005
006
007
008
009
010
011054
055
056
057
058
059
060
061
062
063
064
065
066
067
068
069
070
071
072
073
074
075
076
077
078
079
080
081
082
083
084
085
086
087
088
089
090
091
092
093

Face Sketch Synthesis by Style Transfer with Local Features

Anonymous ICCV submission

Paper ID 612

Abstract

Face sketch synthesis is challenging as it is difficult to generate sharp and detailed textures. In this paper, we propose a new framework based on deep neural networks. Imitating the process of how artists draw sketches, our framework synthesizes face sketches in a cascaded manner in which a content image is first generated that outlines the shape of the face and key facial features, and textures and shadings are then added. We utilize a Fully Convolutional Neural Network (FCNN) to create the content image, and propose a style transfer approach based on local features to append textures. The local feature, what we call pyramid column feature, is a set of features at different convolutional layers corresponding to the same local sketch image patch. We demonstrate that our pyramid column feature can not only preserve more sketch details than common style transfer method but also surpass traditional patch based approach. Quantitative and qualitative evaluations suggest that our framework outperforms other state-of-the-arts methods. In addition, despite of the small training data, our model shows great generalization ability across different datasets and can generate reasonable results under practical situations.

1. Introduction

Face sketch synthesis has drawn a great attention from the community in recent years because of its wide range of applications. For instance, it can be exploited in law enforcement for identifying suspects from a mug shot database consisting of both photos and sketches. Besides, face sketch has also been widely used for entertainment purpose. For example, filmmakers could employ face sketch synthesis technique to ease the cartoon production process.

Unfortunately, there exists no easy solution to face sketch synthesis due to the big stylistic gap between photos and sketches. In the past two decades, a number of exemplar based methods [15, 12, 20, 21] were proposed. In

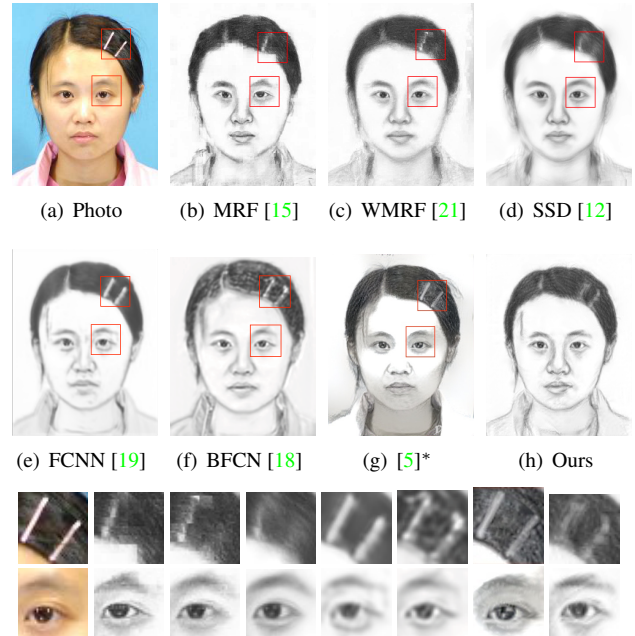


Figure 1. Face sketches generated by existing methods and the proposed method. Our method can not only preserve both hair and facial content, but also maintain sharp textures. (g)* is obtained from deep art website¹ by using a photo as content and a sketch from training set as style.

these methods, an input photo is divided into patches and candidate sketches for each photo patch are selected from a training set. The main drawback of such kind of methods is that if there is no patch in the training data being similar to a patch of test image, loses of some contents will be observed in the final results. For example, the sketches in the first row of Fig. 1 fail to keep the hairpins. Besides, some methods [12, 21] clear away the textures when they try to eliminate the inconsistency between neighboring patches. Another potential risk is that the result may not look like the original photo, e.g. left eye in Fig. 1(b). Recently, approaches [18, 19] based on convolutional neural network (CNN) were developed to solve these problems. Since these models directly generate sketches from photo, structures and contents

¹<https://deeprart.io/>

of photos can be maintained. However, pixel wise loss function as adopted in these approaches will lead to a blurring artifacts as shown in Fig. 1(e) and 1(f). The pixel wise loss can not perceive the texture structure in sketches. The popular neural style transfer provides a better solution for texture synthesis. But there are two obstacles towards directly applying such kind of method. First, it is easily influenced by illumination of the photo, see the face of Fig. 1(h). Second, it needs a style image to give the global statistics of textures. If the given style doesn't coincide with target sketch (which we don't have), some side effects will occur, *e.g.* the nose in Fig. 1(h). Extensive experiment and discussion is given in Section 5.1.

For an artist, the procedure of sketching a face usually starts with outlining the shape of the key facial features like the nose, eyes and mouth. Textures and shadings are then added to regions such as hair, lips, and bridge of the nose to give sketches a specific style. Inspired by this and neural style transfer [4], we propose a new framework for face sketch synthesis that overcomes the aforementioned limitations. In our method, the outline of a face is delineated by a feed-forward neural network, and textures and shadings are then added by a style transfer approach. Specifically, we design a new architecture of Fully Convolutional Neural Network (FCNN) which contains inception layers [13] and convolution layers with batch normalization [6] to outline the face (Section 4.1). For the texture part, we first divide the feature maps of the target sketch in each layer into a fixed size grid and combine features from different layers but at the same grid location into a pyramid feature column. These pyramid feature columns can be generated by local sketch patches from the training set. We find these sketch patches by matching the test image patch to the image-patch pairs in training set (Section 4.2). A target style is then computed by assembling these pyramid columns. Our approach is superior to the current state-of-the-art methods (Section 5.2) in that

- It is capable of generating more stylistic sketches without introducing over smoothing artifacts.
- It can well preserve the content of the test photo.

2. Related Work

2.1. Face Sketch Synthesis

Based on the taxonomy of previous studies [12, 21], face sketch synthesis methods can be roughly categorized into profile sketch synthesis methods [1, 2, 16] and shading sketch synthesis methods [9, 12, 14, 15, 19, 20, 21]. Compared with profile sketches, shading sketches are more expressive and thus more preferable in practice. Based on the assumption that there exists a linear transformation between a face photo and a face sketch, the method in [14] computes

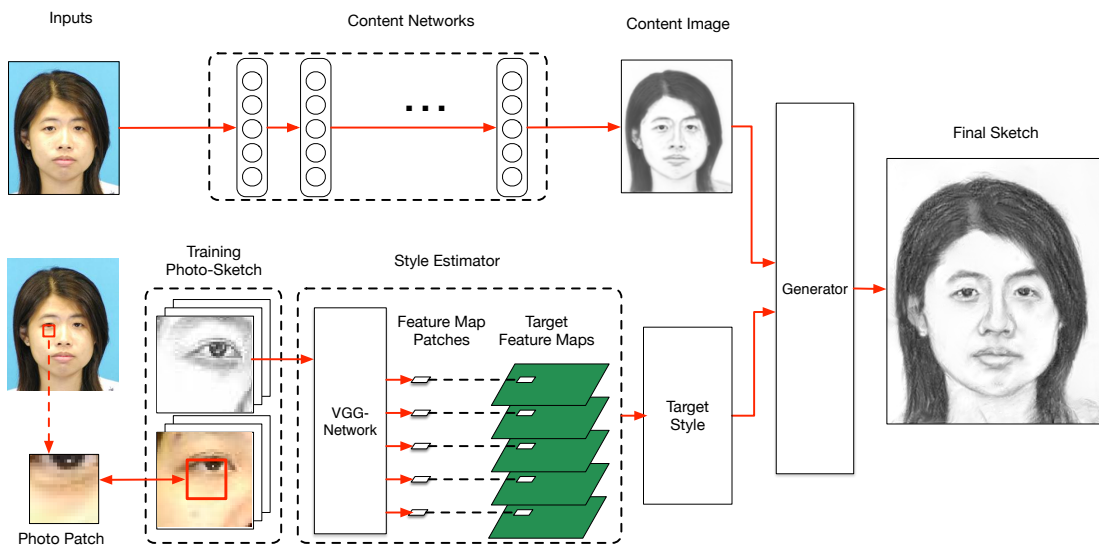
a global eigen-transformation for synthesizing face sketches from face photos. This assumption, however, does not always hold since the modality of face photos and that of face sketches are quite different. Fortunately, Liu et al. [9] found that the linear transformation holds better locally and therefore they proposed a patch based method to perform sketch synthesis. A MRF based method [15] was proposed to preserve large scale structures across sketch patches. Variants of the MRF based methods were introduced in [20, 21] to improve the robustness to lighting and pose, and to render the ability of generating new sketch patches. In addition to these MRF based methods, approaches based on guided image filtering [12] and feed-forward convolutional neural network [19] are also found to be effective in transferring photos into sketches. A very recent work similar to ours is done by Zhang et al. [18]. They proposed a two branch FCNN to learn content and texture respectively and then fusion them through a face probability map. Although their results are impressive, the sketch texture is not natural and the facial components are smoothed.

2.2. Style Transfer with CNN

Texture synthesis has long been a challenging task. Traditional method can only imitate repetitive patterns which has a strong limitation. Recently, Gatys et al. [4, 5], studied the use of CNN in style representation (including texture and color) where a target style is computed based on features extracted from an image using the VGG-Network and an output image is generated by minimizing the difference between its style and the target style. It can transfer a given style to a given images, and provide impressive results. Justin et al. [7] further accelerated this process by learning a feed forward CNN in the training stage. These methods represent textures by a multi-scale gram matrix of feature maps. Since gram matrix cares about global statistics, if the style is very different from the photo, it usually breaks the local structures. Although it may not be a big deal in artistic style, it can't be tolerated in face sketch synthesis because people are sensitive to the distortion of key features of faces. In [3], Chen and Schmidt propose a different patch based style transfer method which is better at capture local structures but still not good enough to this task. Our style transfer mechanism is inspired by but different from these works [4, 5, 7] in that our target style is extracted from many image patches rather than from a single style image. Note that there usually does not exist a single style image in the training set that matches all properties of the test image.

3. Motivation of Pyramid Feature Column

Following the practice of [5], we use the gram matrix of VGG-19[11] feature maps as our style representation. Denote the vectorized feature map of the final sketch \mathcal{X} in the

216
217
218
219
220
221
222
223
224
225
226
227
228
229
230
231
232
233

234 Figure 2. The proposed method contains two branches which take a photo aligned by the eyes as inputs. The content network outputs a
 235 content image and the style estimator generates a target style. The final sketch is generated by combining the target style with the content
 236 image.

237
 238
 239 l th layer by $F^l(\mathcal{X})$. A gram matrix is the inner product between the feature maps in l th layer

$$240 \quad G_{ij}^l(\mathcal{X}) = \sum_{k=1}^{M_l} F_{ik}^l(\mathcal{X}) F_{jk}^l(\mathcal{X}) \quad (1)$$

241 where $G^l(\mathcal{X}) \in \mathcal{R}^{N_l \times N_l}$, M_l is the height times width of
 242 the feature map $F^l(\mathcal{X})$, and N_l is the number of feature
 243 maps in the l th layer. Since $G_{ij}^l(\mathcal{X})$ is an inner product of
 244 feature maps, a gram matrix is actually a summary statistics
 245 of feature maps discarding the spatial information. Al-
 246 though we still not clear what these values exactly mean, we
 247 can safely make an assumption that it at least captures the
 248 density distribution of a sketch. In other word, if the given
 249 sketch style has much less hair than the test image, the
 250 generated sketch \mathcal{X} will possibly be unnaturally bright than a
 251 natural sketch. Experiments in Section 5.1 also prove this.
 252 Thus it is important to keep the given style sketch roughly
 253 the same with test image statistically. On the other hand,
 254 there usually does not exist a candidate image in the train-
 255 ing set that perfectly matches a given test photo in style.
 256 We hence propose a feature level patch based method to
 257 estimate the style of the final sketch. Each feature patch
 258 corresponds to a sketch patch. The reason why we can separate
 259 features into patches comes from [8]. The feature vectors at
 260 different position of feature map can be viewed as indepen-
 261 dent samples when we use gram matrix.

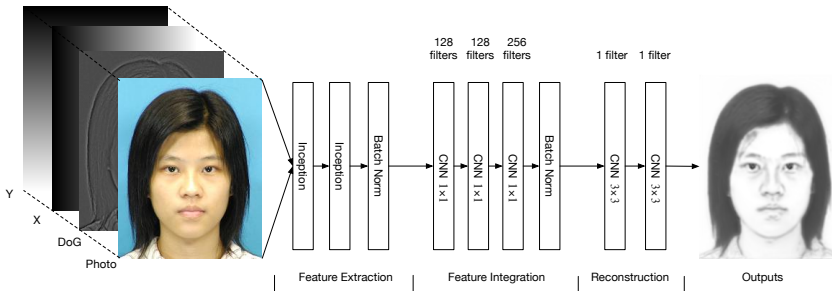
262 4. Methodology

263 Our method can be classified as a shading synthesis
 264 method. The steps of our method are summarized in Fig. 2.

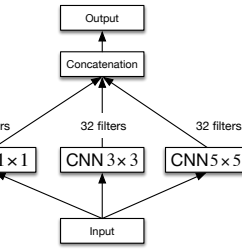
265 First, a preprocessing step as described in [15] is carried
 266 out for all photos and sketches in a training set to align the
 267 centers of two eyes. A test photo \mathcal{I} is then fed into two
 268 branches, namely the content network and the style gen-
 269 erator. The content network converts the test photo into a
 270 content image \mathcal{C} , where the shape of the face are outlined
 271 with the key facial features preserved, such as noses, eyes,
 272 mouths and hair. The style estimator takes a 16×16 local
 273 patch from test photo as input and searches photo-sketch
 274 pairs in the training set to find a target sketch patch S_{ij}
 275 ((i, j) denotes the patch location). Each S_{ij} with its sur-
 276 rounding region can generate a pyramid feature column U_{ij} .
 277 Combining all U_{ij} , we can get the target style features of \mathcal{I} ,
 278 i.e., \tilde{U} . Given \mathcal{C} and \tilde{U} , we can generate a sketch \mathcal{X} that
 279 combines the content information in \mathcal{C} with the style repre-
 280 sentation \tilde{U} following the iterative procedure in [5].

281 4.1. Content Image Generation

282 Our content network architecture is shown in Fig. 3. To-
 283 gether with the test photo, we feed two extra channels con-
 284 taining spatial information (i.e., x and y coordinates) and a
 285 difference of Gaussian (DoG) image into the content net-
 286 work. As pointed out in [15], face sketch synthesis algo-
 287 rithms benefit from integrating features from multiple res-
 288 olutions. We employ an inception module inspired by the
 289 GoogLeNet [13] to extract features. It concatenates fea-
 290 ture maps generated from filters with different spatial res-
 291 olutions. Our inception unit contains 3 different size of filters
 292 (1×1), (3×3) and (5×5) (see Fig. 3(b)). Then, the output
 293 features are fed to a three-layer-CNN for feature integra-
 294 tion, where the size of all filters are fixed at 1×1 . Finally, the



(a) The architecture of content network



(b) Inception module

Figure 3. Illustration of the content network for generating a content image. The numbers above the building block denote the number of CNN filters. (a) The architecture of content network. (b) The inception module in (a) contains three groups of filters with different sizes.

integrated features are used to reconstruct the content map by a two-layer-CNN with the filter size being 3×3 . Because L_1 -norm is better at preserving details than L_2 -norm, we use the L_1 -norm between the generated content image \mathcal{C} and ground truth sketch S as the loss function, see Equ. 2.

$$\mathcal{L}_s = \frac{1}{N} \sum_{i=1}^N \|\mathcal{C}_i - S_i\| \quad (2)$$

where N is the number of photos.

4.2. Pyramid Feature Column

Fig. 4 shows an example of the pyramid feature column. Denote the feature maps (of the l th layer) used to estimate the style of the final sketch by A^l . In our feature patch based method, we divide A^l into a fixed size of grid. Due to the different feature map size, the sizes of the feature patches at layer $conv1_1$, $conv2_1$, $conv3_1$, $conv4_1$ and $conv5_1$ are 16×16 , 8×8 , 4×4 , 2×2 and 1×1 . The photos and sketches are resized to 288×288 thus the size of grid is 18×18 . Grouping feature map patches having the same grid indexes (i, j) at different layers together, we get a pyramid feature column U_{ij} . To estimate U_{ij} , a sketch patch in the training set is fed to the VGG-Network and a pyramid column is composed of the resulting feature maps. This process consists of two steps: (1) find a matching sketch patch S_{ij} from the training set for U_{ij} and (2) feed S_{ij} to VGG-Network and extract U_{ij} from the resulting feature maps.

Find Matching Sketch Patch Similar to previous works [15, 21], we examine the similarity of test photo patch and train photo patches to find a matching sketch S_{ij} for U_{ij} . Denote the train photo patch set as P , given a test photo patch T'_{ij} , the target sketch patch S_{ij} is found by

$$S_{ij} = \phi(\min_{T_{mn}^k \in P} f(T_{mn}^k, T'_{ij})) \quad (3)$$

$$m = i + \Delta x, n = j + \Delta y \quad (4)$$

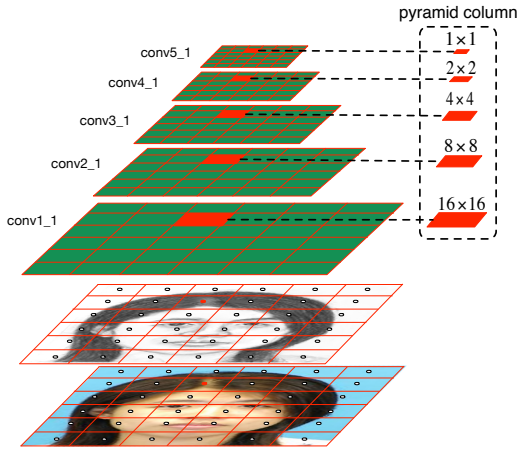


Figure 4. Illustration of pyramid feature column. Feature maps of the final sketch A^l are divided into a fixed 18×18 grid. A pyramid column U_{ij} consists of feature map patches at different layer having the same grid indexes (i, j) .

where T_{mn}^k is the photo patch of the k th image at (m, n) in training set, ϕ is a one-to-one mapping between photo patch and sketch patch, Δx and Δy is the shift of (m, n) around (i, j) . The function f measures the discrepancy between T_{mn}^k and T'_{ij} . Because we only need the test photo patch and train photo patch have a similar appearance, we simply use MSE as f here.

Estimate Pyramid Feature Column After we get S_{ij} , we can compute the corresponding pyramid feature column U_{ij} . Although the feature column can be generated by a 16×16 patch, padding zeros is not a good idea. Therefore, we will make use of the surrounding area of S_{ij} to compute U_{ij} . According to the architecture of VGG-19, the receptive field of $conv5_1$ is 132 without padding. To get 16×16 patches, we will need a 144×144 region \mathcal{R} containing 81 patches in total. S_{ij} should be at the center of \mathcal{R} , i.e. S_{55} with respect to the grids of \mathcal{R} . For those border part where

we can't find a region centered at S_{ij} , we just find another region \mathcal{R}' which has the biggest intersection with the should be region \mathcal{R} (the blue box in Fig. 5). The S_{55} in \mathcal{R} should be S'_{pq} in \mathcal{R}' ((p, q) is calculated according to different conditions). The feature column U_{55} in \mathcal{R} or U_{pq} in \mathcal{R}' is the estimated pyramid feature column.

Allocating all these feature columns to its original patch location (i, j) , we can get the final feature maps \tilde{U} and use it to compute gram matrix.

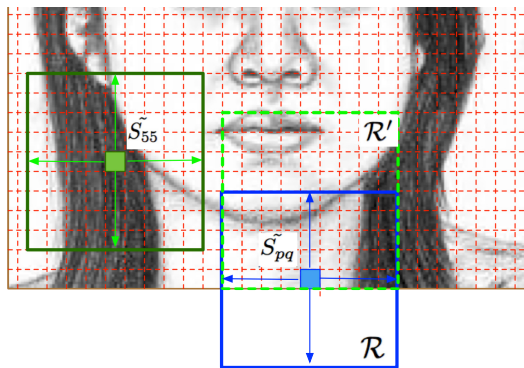


Figure 5. Find a region \mathcal{R} centered at S_{ij} . If \mathcal{R} is inside the image, S_{ij} should be the center patch of \mathcal{R} , see the left region. Otherwise, we need to find \mathcal{R}' inside the image which has the biggest intersection with \mathcal{R} , see the right part. Suppose the indexes of S_{ij} inside \mathcal{R}' is (p, q) , then U_{pq} is the corresponding feature column.

4.3. Loss Function of Sketch

The same as [5], our loss function has a style loss and content loss. In addition we add a component loss to enhance the key facial components. The total loss is

$$\mathcal{L}_t(\mathcal{X}) = \alpha \mathcal{L}_c + \beta_1 \mathcal{L}_s + \beta_2 \mathcal{L}_k \quad (5)$$

We minimize the loss function by updating the target sketch \mathcal{X} without changing the VGG parameters.

The content loss is defined based on the difference between the feature map of the sketch and the content image at layer conv1_1:

$$\mathcal{L}_c(\mathcal{X}) = \|F^{\text{conv1_1}}(\mathcal{X}) - F^{\text{conv1_1}}(\mathcal{C})\|_2^2. \quad (6)$$

And the style loss is the difference between the gram matrix of the final sketch and the target gram matrix

$$\mathcal{L}_s(\mathcal{X}) = \sum_{l \in L_s} \frac{1}{M_l^2 N_l^2} \|G^l(\mathcal{X}) - G^l(\tilde{U})\|_2^2 \quad (7)$$

where N_l denotes the number feature maps at layer l , and M_l is the feature map width times height.

To better transfer styles of the key facial components, we employ a component loss to encourage the key component style of the final sketch being the same as the target

key component style. Since two eyes are placed at fixed positions, the key components lie roughly within a rectangular region taking the positions of two eyes as vertices. Key component style is given by gram matrices calculated within feature map regions \mathcal{K} corresponding to the key components. These regions are specified by pyramid feature columns U_{ij} whose C_{ij} are inside \mathcal{K} . We take out \mathcal{K} and calculate the corresponding gram matrix loss as the component loss

$$\mathcal{L}_k(\mathcal{X}) = \sum_{l \in L_s} \frac{1}{\hat{M}_l^2 N_l^2} \|\hat{G}^l(\mathcal{K}) - \hat{G}^l(\tilde{U}_k)\|_2^2 \quad (8)$$

where \hat{M}_l denotes height times width of \mathcal{K} .

4.4. Implementation Details

VGG-19 Parameters Since the VGG-Network is originally designed for color images, while sketches are gray scale images, we modify the first layer of VGG-Network for gray scale images by setting the filter weights to

$$W^k = W_r^k + W_g^k + W_b^k \quad (9)$$

where W_r^k , W_g^k , and W_b^k are weights of the k th filter in the first convolutional layer for the R, G and B channels respectively, and W^k is the weight of the k th filter in the first convolutional layer of our modified network.

Data Partition CUHK has 88 training photos and 100 test photos, and AR has 123 photos. Our training set is composed of the 88 training photos of CUHK and 100 photos from AR. When training the content network, 10% of the training set are taken out as validation set. All the 188 photo-sketch pairs are used to generate target sketch.

Training content network The input photo-sketch pairs are aligned by the facial landmarks of eyes, and all images are resized to 200×256 . A mirror padding is carried out before the convolution operation when necessary to ensure the output feature map is the same size as the input. Adadelta [17] is used as the optimizer because it is stable and much faster than others.

Sketch Generation In all experiments, we resize test photos and photo-sketch pairs in the training set to a fixed size of 288×288 . The final sketch is obtained by resizing the resulting sketch back to the original size. The size of \mathcal{K} is 48×48 , $\alpha = 0.004$, $\beta_1 = 1$ and $\beta_2 = 0.1$. The minimization is carried out using L-BFGS. Instead of using random noises, we use the content image as a starting point, which will make the optimization process converge much faster.

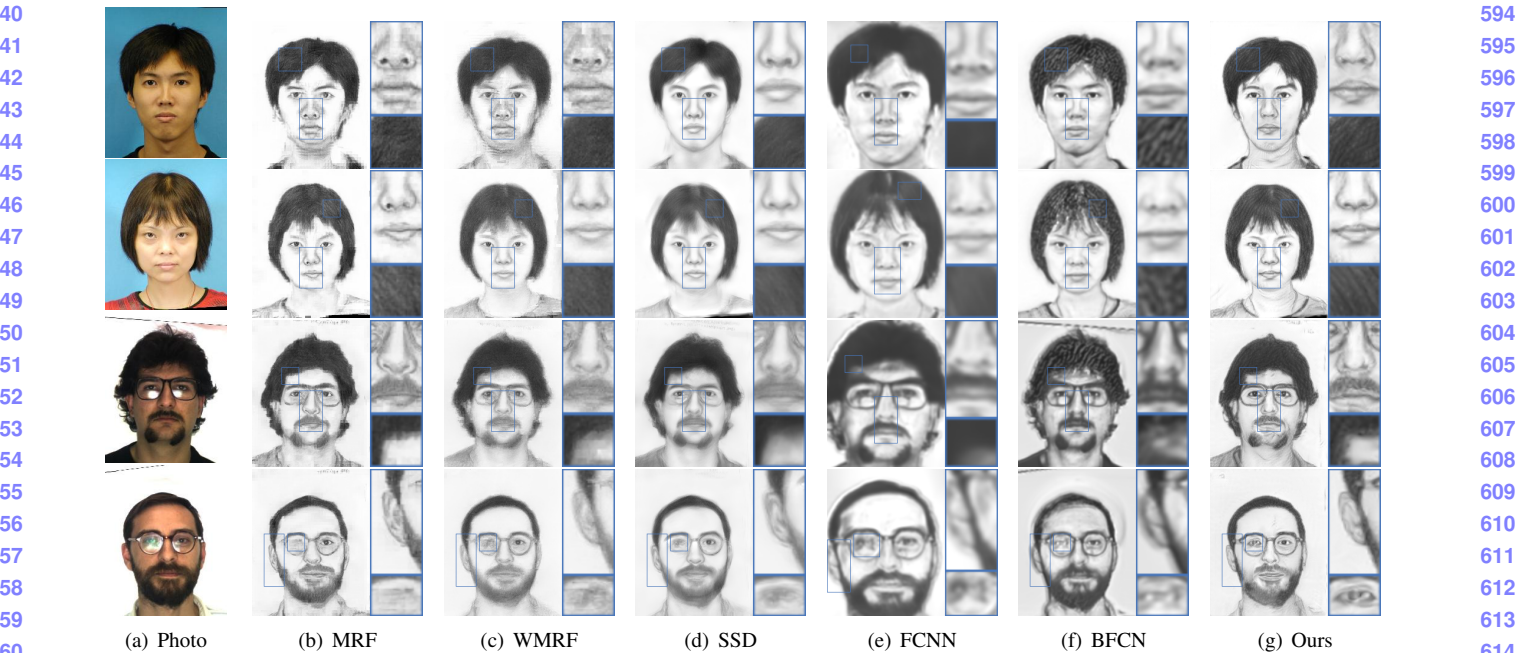


Figure 6. Examples of qualitative evaluation on CUHK (first two rows) and AR (last two rows). (a) The sketches drawn by artists. (b) MRF [15] (c) WMRF [21] (d) SSD [12] (e) FCNN [19] (f) BFCN [18] (g) Ours. The proposed method preserves more texture details, for example in the hair and nose. It is also best at keeping the origin structures of photos, such as the glasses.

5. Experiments

We evaluate the performance of the proposed method against other state-of-the-art methods on the CUHK student dataset [15] and the AR dataset [10]. We compare the results of our method against other 6 methods including traditional approaches and recent deep learning models. After discussing the disadvantages of previous quantitative evaluation criteria, we introduce the Normalized Gram Matrix Difference (NGMD) as a new evaluation tool. We believe that NGMD is more effective and will greatly promote the sketch qualities in future work.

5.1. Style Transfer Evaluation

Although style transfer has shown remarkable performance in artistic style, it can't be directly applied to face sketch synthesis, see Fig. 1(h). The generated sketch is greatly influenced by illumination of original photo and doesn't look like sketch at all. To prove our assumption in Section 3 that gram matrix captures the density distribution of sketch, we replace the original RGB photo with content image generated by our content network. We selected 3 sketch styles with different amount of hairs and see how it influences the result. Fig. 7 shows a clear relationship between the hair amount of sketch and pixel intensities of sketch result. The facial key parts in Fig. 7(c) and 7(d) are missed. Therefore, even with a content structure, the original style transfer is still not suitable for elaborate task. However, if the style image has a similar structure with test

photo, for example Fig. 7(b), the results can be quite good. This inspires our feature patch based method. Image patch method is not considered because it will introduce patch inconsistency as discussed in Section 2.

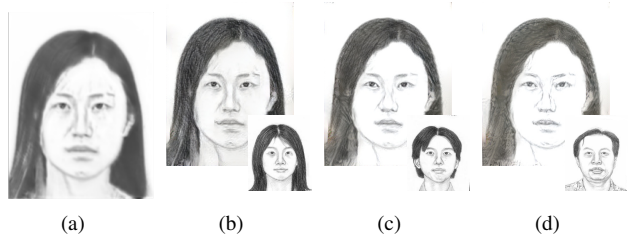


Figure 7. (a) is the content image generated by our content network. (b), (c) and (d) are generated by different styles. It can be seen that when the hair decreases the generated sketch becomes brighter.

5.2. Sketch Generation

Fig. 6 shows the comparison between our methods and many other approaches. The first two rows are from CUHK test set, and the last two are from AR. We can see that our method can generate more stylistic sketches than others. For example, in the hair part, only MRF, BFCN and the proposed method can generate obvious textures. However, the texture of MRF is not continuous in the border part and introduce many other artifacts, and the texture of BFCN doesn't look like human strokes. Both WMRF and SSD in-

648
649
650
651
652
653
654
655
656
657
658
659
660
661
662
663
664
665
666
667
668
669
670
671
672
673
674
675
676
677
678
679
680
681
682
683
684
685
686
687
688
689
690
691
692
693
694
695
696
697
698
699
700
701
troduce over smoothing effect and FCNN is not able to give clear textures. Our method can not only generate textures for hairs and mustache but also shadings, for example the nose part.

On the other hand, only BFCN and the proposed method can handle structures decorated on the face well, for example the glasses of the last two row. MRF, WMRF and SSD are exemplar based method so they can't handle something different from training set, the glass edges of them are not complete. FCNN, BFCN and our method generate the image content by CNN, so they can handle the original photo structures well. But both FCNN and BFCN care nothing about the textures of facial part, so their results are not good considering the face part. In contrast, our method can well maintain the image content and attach textures similar to human paintings.

5.3. Quantitative Results

Methods	AR			CUHK		
	R1	R5	R10	R1	R5	R10
FCNN	-	-	-	81%	96%	97%
MRF	97.5%	97.5%	100%	83%	96%	96%
WMRF	97.5%	97.5%	100%	83%	97%	98%
SSD	96.7%	97.5%	100%	87%	97%	98%
Ours	98.4%	98.4%	100%	87%	98%	99%

Table 1. Recognition rate on benchmark datasets. The best performance is colored in red.

Sketch Recognition Sketch synthesis methods are usually evaluated quantitatively via the face sketch recognition task [12, 15, 19, 21]. If an algorithm achieves higher sketch recognition rates, it suggests that this method is more effective in synthesizing sketches. We adopt the widely used PCA based recognition method with “rank-1 (R1)”, “rank-5 (R5)” and “rank-10 (R10)” criteria [15] where “rank n ” measures the rate of the correct answer in the top n best matches. The results of different methods are shown in Table 1. Our method achieves the best performance against all other methods in the “R1” and “R5” tests.

However, such kind of evaluation is not effective since every one is close to 100%, and more importantly, it can't guide our research effort. Zhang *et al.* [19] proposed a Multiscale Pixel-wise Reconstruction Loss (MPRL). Although we agree that if MPRL is zero, the generated sketches will be exactly the same with ground truth, there are two reasons why it is not a good criteria. First, experiment results of [19, 18] show that L_2 -norm would give blurry sketches. Second, the ground truth draw by human usually doesn't correspond exactly with photos, thus difficult for algorithms to reach the ground truth.

Meanwhile, human can often be able to tell whether a sketch is generated by algorithms or drawn by artists just

from a quick glance without examining details. This indicates that there exists a big gap between the style of algorithm-generated sketches and that of those drawn by artists. And we need a criteria which can quantitatively measure such gap.

Normalized Gram Matrix Difference (NGMD) To quantitatively evaluate the style similarity between a generated sketch and the sketch drawn by a real artist, we employ the normalized gram matrix difference (NGMD) between the generated sketch \mathcal{X} and the drawn sketch $\tilde{\mathcal{X}}$:

$$D_s^l(\mathcal{X}, \tilde{\mathcal{X}}) = \frac{\|G^l(\mathcal{X}) - G^l(\tilde{\mathcal{X}})\|_2}{\|G^l(\tilde{\mathcal{X}})\|_2} \quad (10)$$

where $l \in L_s$. The smaller the NGMD value is, the more similar \mathcal{X} and $\tilde{\mathcal{X}}$ are.

It is exciting how well NGMD match our intuition, see Fig. 6. The results of [19] can roughly outline the sketches but can't add textures, thus they got a high NGMD in Table 2. The results of MRF [15] and WMRF [21] are more similar to hand drawn sketches in style since these exemplar based approaches use patches of hand drawn sketches to make up the target sketch. That is why they have a smaller NGMD value. Inheriting the ability of denoising, the filtering based approach [12] is good at suppressing noises in the results. However, it is also likely for this method to over-smooth the results, which will deteriorate the texture, thus its NGMD value is higher than WMRF.

5.4. Generalization Evaluation

In this part, we will evaluate the generalization ability of our model in two aspects.

Light and Pose Invariance As discussed in [20], light and pose change may influence the result a lot. We choose several photos from [20] and compare our results with MRF(extended) [20] and BFCN [18]. Fig. 8 shows the comparison. Our proposed method is not influenced by pose and light change and can still generate good textures under lab environment.

Real World Photos We further tested the robustness of our model on some real world photos, see Fig. 9. The first two rows are Chinese celebrity faces from [20], and the latter two comes from the web. Since the test photo may not be well aligned, we just turn off the component loss. The parameters we use here are $\alpha = 0.004$, $\beta_1 = 1$, $\beta_2 = 0$. Although the background is clutter and the positions of faces are not strictly constrained. The hair style of our results are still clear and sharp, while FCNN and BFCN can't produce good textures.

756	Methods	AR					CUHK					810	
757		conv1_1	conv2_1	conv3_1	conv4_1	conv5_1	758	conv1_1	conv2_1	conv3_1	conv4_1	conv5_1	811
759	FCNN	-	-	-	-	-	759	0.009	0.110	0.080	9.43	1.49	812
760	MRF	0.0043	0.009	0.033	0.12	0.28	760	0.010	0.014	0.047	0.13	0.18	813
761	WMRF	0.0053	0.027	0.085	0.19	0.29	761	0.010	0.052	0.052	0.27	0.19	814
762	SSD	0.0056	0.036	0.110	1.90	0.28	762	0.009	0.102	0.070	3.32	0.24	815
763	Ours	0.0035	0.008	0.029	0.08	0.17	763	0.007	0.012	0.033	0.07	0.12	816

Table 2. Averaged NGMD value of different methods at different level on AR and CUHK datasets. A smaller NGMD indicates the generated texture is more similar to ground truth.

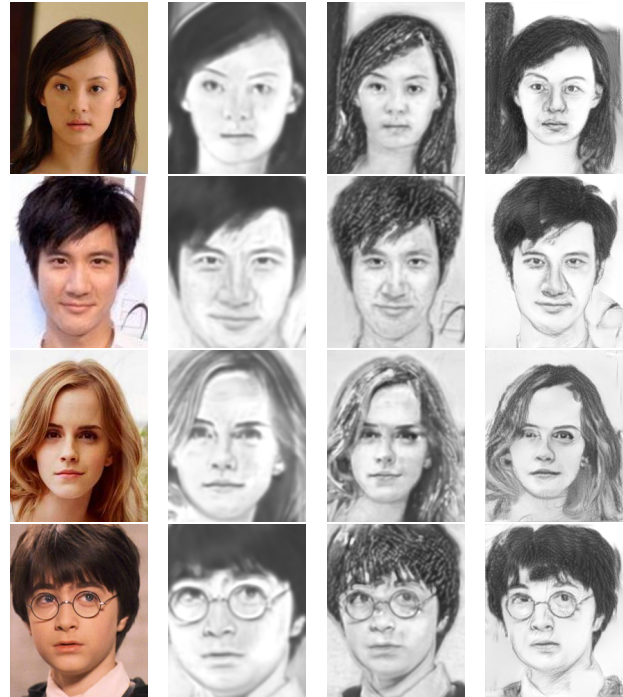


(a) Photo (b) MRF(extend) (c) BFCN (d) Ours

Figure 8. Experiment with different light and pose. Our results are little affected by light and pose change.

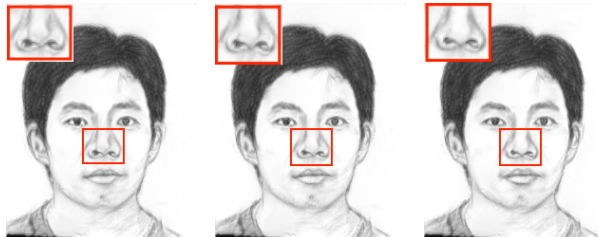
5.5. Effectiveness of the model

The loss function we minimize during the generation of sketches contains three terms for content, style and key components respectively. The term \mathcal{L}_k regularizes the results by encouraging the style extracted from the key component regions in the training set to be placed into the key components region of the results, which helps generate better results around these components (see Fig. 10). To better understand how style influences the final sketch, we smoothly change the emphasis on style by adjusting β_1 and β_2 while keeping α fixed. Fig. 11 indicates that the sketch with style transferred contains more texture and is more like a drawn sketch. The Theano implementation of the proposed method takes approximately 100 seconds to generate a sketch on a GeForce GTX TITAN X platform. The bottle



(a) Photo (b) FCNN (c) BFCN (d) Ours

Figure 9. Experiments with real world photos. Our method can still get better results under practical situations.



(a) (a) $\beta_2 = 0.001$ (b) (b) $\beta_2 = 0.01$ (c) (b) $\beta_2 = 0.1$

Figure 10. Comparison between results with different weight of \mathcal{L}_k regulation. With the increase of β_2 the distortion of nose becomes less.

neck lies in the style transfer which requires feeding \mathcal{X} to the VGG-Network to estimate targeting feature maps and to calculate the gradient of Eq. (5), which is computationally



$\beta_1 = 0$ $\beta_1 = 10^{-3}$ $\beta_1 = 10^{-2}$ $\beta_1 = 0.1$ $\beta_1 = 1$ $\beta_1 = 10^3$
 $\beta_2 = 0$ $\beta_2 = 10^{-4}$ $\beta_2 = 10^{-3}$ $\beta_2 = 0.01$ $\beta_2 = 0.1$ $\beta_2 = 10^2$

Figure 11. Final results for sketch synthesis with fixed $\alpha = 0.004$ and different β_1, β_2 values.

intensive.

6. Conclusion

This paper proposed a novel face sketch synthesis method inspired by the procedure of artists drawing sketches. In our method, the outline of the face is delineated by a content network and the style extracted from sketches drawn by artists are transferred to generate a final sketch. Quantitative evaluations on face sketch recognition and style similarity measure demonstrate the effectiveness of the proposed algorithm for face sketch synthesis and style transferring. Our future work will investigate accelerating technique to reduce the running time and achieve real time face sketch synthesis with style transfer.

References

- [1] I. Berger, A. Shamir, M. Mahler, E. Carter, and J. Hodgins. Style and abstraction in portrait sketching. *ACM Transactions on Graphics (TOG)*, 32(4):55, 2013. [2](#)
- [2] H. Chen, Y.-Q. Xu, H.-Y. Shum, S.-C. Zhu, and N.-N. Zheng. Example-based facial sketch generation with non-parametric sampling. In *Computer Vision, 2001. ICCV 2001. Proceedings. Eighth IEEE International Conference on*, volume 2, pages 433–438. IEEE, 2001. [2](#)
- [3] T. Q. Chen and M. Schmidt. Fast patch-based style transfer of arbitrary style. *CoRR*, abs/1612.04337, 2016. [2](#)
- [4] L. Gatys, A. S. Ecker, and M. Bethge. Texture synthesis using convolutional neural networks. In *Advances in Neural Information Processing Systems*, pages 262–270, 2015. [2](#)
- [5] L. A. Gatys, A. S. Ecker, and M. Bethge. A neural algorithm of artistic style. *arXiv preprint arXiv:1508.06576*, 2015. [1, 2, 3, 5](#)
- [6] S. Ioffe and C. Szegedy. Batch normalization: Accelerating deep network training by reducing internal covariate shift. *CoRR*, abs/1502.03167, 2015. [2](#)
- [7] J. Justin, A. Alexandre, and F.-F. Li. Perceptual losses for real-time style transfer and super-resolution. In *European Conference on Computer Vision*, pages 694–711, 2016. [2](#)
- [8] Y. Li, N. Wang, J. Liu, and X. Hou. Demystifying neural style transfer. *CoRR*, abs/1701.01036, 2017. [3](#)
- [9] Q. Liu, X. Tang, H. Jin, H. Lu, and S. Ma. A nonlinear approach for face sketch synthesis and recognition. In *IEEE Computer Society Conference on Computer Vision and Pattern Recognition*, volume 1, pages 1005–1010. IEEE, 2005. [2](#)
- [10] A. Martinez. R. benavente. the AR face database. Technical report, CVC Tech. Report, 1998. [6](#)
- [11] K. Simonyan and A. Zisserman. Very deep convolutional networks for large-scale image recognition. *arXiv preprint arXiv:1409.1556*, 2014. [2](#)
- [12] Y. Song, L. Bao, Q. Yang, and M.-H. Yang. Real-time exemplar-based face sketch synthesis. In *ECCV*, pages 800–813, 2014. [1, 2, 6, 7](#)
- [13] C. Szegedy, W. Liu, Y. Jia, P. Sermanet, S. Reed, D. Anguelov, D. Erhan, V. Vanhoucke, and A. Rabinovich. Going deeper with convolutions. In *Proceedings of the IEEE Conference on Computer Vision and Pattern Recognition*, pages 1–9, 2015. [2, 3](#)
- [14] X. Tang and X. Wang. Face sketch synthesis and recognition. In *IEEE International Conference on Computer Vision*, pages 687–694. IEEE, 2003. [2](#)
- [15] X. Wang and X. Tang. Face photo-sketch synthesis and recognition. *IEEE Transactions on Pattern Analysis and Machine Intelligence*, 31(11):1955–1967, 2009. [1, 2, 3, 4, 6, 7](#)
- [16] Z. Xu, H. Chen, S.-C. Zhu, and J. Luo. A hierarchical compositional model for face representation and sketching. *IEEE Transactions on Pattern Analysis and Machine Intelligence*, 30(6):955–969, 2008. [2](#)
- [17] M. D. Zeiler. ADADELTA: an adaptive learning rate method. *CoRR*, abs/1212.5701, 2012. [5](#)
- [18] D. Zhang, L. Lin, T. Chen, X. Wu, W. Tan, and E. Izquierdo. Content-adaptive sketch portrait generation by decompositional representation learning. *IEEE Transactions on Image Processing*, 26(1):328–339, 2017. [1, 2, 6, 7](#)
- [19] L. Zhang, L. Lin, X. Wu, S. Ding, and L. Zhang. End-to-end photo-sketch generation via fully convolutional representation learning. In *Proceedings of the 5th ACM on International Conference on Multimedia Retrieval*, pages 627–634. ACM, 2015. [1, 2, 6, 7](#)
- [20] W. Zhang, X. Wang, and X. Tang. Lighting and pose robust face sketch synthesis. In *Computer Vision–ECCV 2010*, pages 420–433. Springer, 2010. [1, 2, 7](#)
- [21] H. Zhou, Z. Kuang, and K.-Y. K. Wong. Markov weight fields for face sketch synthesis. In *IEEE Conference on Com-* [918](#)
- [919](#)
- [920](#)
- [921](#)
- [922](#)
- [923](#)
- [924](#)
- [925](#)
- [926](#)
- [927](#)
- [928](#)
- [929](#)
- [930](#)
- [931](#)
- [932](#)
- [933](#)
- [934](#)
- [935](#)
- [936](#)
- [937](#)
- [938](#)
- [939](#)
- [940](#)
- [941](#)
- [942](#)
- [943](#)
- [944](#)
- [945](#)
- [946](#)
- [947](#)
- [948](#)
- [949](#)
- [950](#)
- [951](#)
- [952](#)
- [953](#)
- [954](#)
- [955](#)
- [956](#)
- [957](#)
- [958](#)
- [959](#)
- [960](#)
- [961](#)
- [962](#)
- [963](#)
- [964](#)
- [965](#)
- [966](#)
- [967](#)
- [968](#)
- [969](#)
- [970](#)
- [971](#)

972		1026
973	puter Vision and Pattern Recognition, pages 1091–1097.	1027
974	IEEE, 2012. 1, 2, 4, 6, 7	1028
975		1029
976		1030
977		1031
978		1032
979		1033
980		1034
981		1035
982		1036
983		1037
984		1038
985		1039
986		1040
987		1041
988		1042
989		1043
990		1044
991		1045
992		1046
993		1047
994		1048
995		1049
996		1050
997		1051
998		1052
999		1053
1000		1054
1001		1055
1002		1056
1003		1057
1004		1058
1005		1059
1006		1060
1007		1061
1008		1062
1009		1063
1010		1064
1011		1065
1012		1066
1013		1067
1014		1068
1015		1069
1016		1070
1017		1071
1018		1072
1019		1073
1020		1074
1021		1075
1022		1076
1023		1077
1024		1078
1025		1079